IEEE Access
Multidisciplinary ⋮ Rapid Review ⋮ Open Access Journal

Received May 4, 2021, accepted May 23, 2021, date of publication May 26, 2021, date of current version June 9, 2021.

Digital Object Identifier 10.1109/ACCESS.2021.3083922

A Collaborative Demand-Controlled Operation Strategy for a Multi-Energy System

MAO YUNSHOU[1], WU JIEKANG[1], (Member, IEEE), WANG RUIDONG[1], CAI ZHIHONG[1], ZHANG RAN[2], CHEN LINGMIN[1], AND ZHANG WENJIE[3]

[1]School of Automation, Guangdong University of Technology, Guangzhou 510006, China
[2]Beijing Aerocim Technology Company Ltd., Beijing 100043, China
[3]Huizhou Power Supply Bureau, Guangdong Power Grid Corporation, Huizhou 516800, China

Corresponding author: Wu Jiekang (wujiekang@163.com)

This work was supported in part by the Guangdong Basic and Applied Basic Research Foundation under Grant 2020B1515130001, and in part by the Innovation and Entrepreneurship Education Projects of Universities in Guangzhou under Grant 2020PT106.

ABSTRACT The multi-energy system is a promising energy-efficient technology to supply electric and thermal energy to end-users simultaneously, which can realize the energy cascade utilization. However, it is challenging to optimize the operation of multi-energy systems due to their inherent structural complexity, as well as the highly coupled nature of multiple energy flows and the uncertainty of renewable energy generation. This paper proposed a collaborative demand-controlled operation strategy for a multi-energy system, which consists of an upper-level model and a lower-level model. In the upper-level model, a robust linear optimization method is adopted to optimize the system operation in a day-ahead stage. In the lower-level model, a stochastic rolling optimization method is applied to achieve a dynamic adjustment to cope with the fluctuation in both renewable electricity generation and electric load. The multiple energy demand-controlled strategy is also applied in the optimal operation strategy to achieve load shifting and to create flexibility in energy demand despite the ''source-load'' imbalance power fluctuation. A case study is carried out and simulation results verify the effectiveness and correctness of the proposed model of the coordinated operation framework.

INDEX TERMS Multi-energy system, robust linear optimization, indoor temperature control, demand response, optimal operation.

I. INTRODUCTION

A multi-energy system is getting increasing attention for it can provide an effective way to supply electric and thermal energy to end-users simultaneously to realize overall energy cascading utilization [1]–[3]. A multi-energy system usually consists of distributed generation units such as wind turbines (WT), photovoltaic (PV) panels, and a combined cooling, heat and power plant. However, due to the highly multi-energy coupling features and renewable power uncertainties, the electric and thermal demand of end-users may not be matched by the multi-energy system. Moreover, the imbalance between distributed generation (DG) and load demand can cause energy to be wasted and further lower the efficiency of energy use. There has been a surge in the need for research on how to optimize the operation of a multi-energy system.

With the high penetration of renewable energy integrated into multi-energy systems, the basic operation strategies, i.e., following electric load and following thermal load tend to reduce the overall performance of the system while meeting the multiple energy balance of supply-side and demand-side. Thus, many researchers have conducted numerous studies on the optimal operation strategy of multi-energy systems and many effective operation strategies are proposed to improve the comprehensive performance of the multi-energy system. The particle swarm optimization approach was used to optimize the multi-energy flows to achieve an optimal operation strategy that can not only increase renewable energy generation rate but also improves energy supply reliability effectively [4], [5]. By optimizing the electric cooling ratio, an operating parameter, through different heuristic algorithms, better matching performance between the DG side and multi-energy demand side could be achieved [6], [7].

Electric energy storage and thermal energy storage were also used in a multi-energy system to deal with the mismatch

The associate editor coordinating the review of this manuscript and approving it for publication was Ravindra Singh.

between electric and thermal demands. A specific improved following the hybrid electric–thermal load was proposed to further improve the primary energy utilization rate [8]. Energy flow modeling in the energy hub of the micro energy grid was proposed and a day-ahead dynamic optimal dispatch model was given to solve the economic dispatch problem. Multiple energy storage systems and demand response schemes were incorporated in the optimization model, further enabling the system to achieve lower daily operating costs [9], [10]. Based on the fair cost allocation using Shapley values, a cooperative scheduling framework incorporating electric and thermal demand response programs was proposed for multi-energy hubs. Characteristics of integrated energy demand response mechanisms on the impact of flexible energy demand had been investigated to further reduce the total operation cost [11]. Multiple energy demand response mechanisms based on elasticity coefficients were proposed to transfers the user load demand, without changing the total energy consumption, thus achieving better economic, energetic, and degree of matching performance in a multi-energy system [12]. However, those above-mentioned energy dispatch models all neglect the uncertainties of DG power outputs and the multi-energy demand of end-users, which cannot guarantee the reliable operation of the multi-energy system in practice.

Nowadays the uncertainties in the energy supply-side and demand-side pose a significant challenge to the stable and reliable operation of the multi-energy system. Several approaches can be used to address those impacts, like stochastic optimization [13], [14], chance-constrained stochastic optimization [15], [16], fuzzy optimization [17], and robust optimization [18]. Zhang *et al.* [19] proposed a bi-stage stochastic model to optimize both facility capacity allocation and the electric cooling ratio as well to improve the integrated performance under several uncertainties in energy supply and demand sides. Onishi *et al.* [20] proposed a stochastic model to optimize the design and operation of a trigeneration system considering the uncertainties of multi-energy demand and the long-term energy prices. Sedighizadeh *et al.* [21] proposed a stochastic multi-objective model to obtain optimal energy management of a multi-energy system with the integration of plug-in hybrid electric vehicles and electric/thermal energy storages. Zhang *et al.* [22] proposed a two-stage robust optimization to coordinate the multiple energy flows in a multi-energy microgrid under multiple uncertainties, and the optimization model is solved by the column and constraint generation algorithm. The optimal operation strategy of a multi-energy microgrid in grid-connected mode and islanded mode could be achieved to promote energy utilization and operating robustness [23].

The traditional demand response or integrated energy demand response is an effective approach to guide the customers in the demand-side to consume energy rationally and wisely, by which the end-users can participate in the process of system optimization and control [24], [25]. Many researchers usually coordinate the electric and thermal load to be interruptible and curtailable loads in the multi-energy system to improve the operating profit or net operating cost. However, load shifting or load curtailment may hamper end-user's benefits. Moreover, the classification of electrical and thermal loads into interruptible and non-interruptible loads is very limited in practical applications.

Through the above-mentioned literature, many scholars have researched coping with uncertainties on the energy demand side and energy consumption side in multi-energy systems, as well as on integrated energy demand response programs. However, few studies have been conducted to combine both of them well for the optimization of system operation at multiple time scales. Therefore, this paper proposes a collaborative operation strategy to coordinate multiple energy demands during day-ahead and intra-day scheduling. Different optimization strategies are proposed to cope with different degrees of supply-side and demand-side uncertainty in different scheduling periods. This paper makes the following contributions:

- A collaborative operation strategy incorporating multiple energy forms, time scales, uncertainties, and demand response programs is proposed in this paper. The proposed operation strategy has high engineering practicality.
- A collaborative operation strategy comprises a two-stage model. The robust linear optimization is applied in the upper model of the day-ahead scheduling and the stochastic rolling optimization is used in the lower model of the intra-day scheduling. Various uncertainties handling and multiple energy demand-controlled programs are jointly combined into the proposed operation framework.
- The management of multiple energy demand-controlled in the day-ahead scheduling and intra-day scheduling can effectively realize loads shifting and create flexibility in thermal demand despite fluctuation in energy supply-side and demand-side.

The rest of the paper is organized as follows: Section 2 introduces the description of a multi-energy system; Section 3 introduces a two-stage collaborative operation strategy and a multiple energy demand-controlled strategy; Section 4 and Section 4 present the case studies and conclusion respectively.

II. DESCRIPTION OF MULTI-ENERGY SYSTEM

A typical framework of a multi-energy system is illustrated in Figure 1. The input ports of system are usually connected to the main grid, natural gas, and different distributed generation units like wind turbines, gas turbines and photovoltaic modules and etc.

The output ports of the multi-energy system can provide electricity, cooling energy, and heating energy simultaneously. Depending on the price of electricity or natural gas, the status of the device, and the weather data, the energy

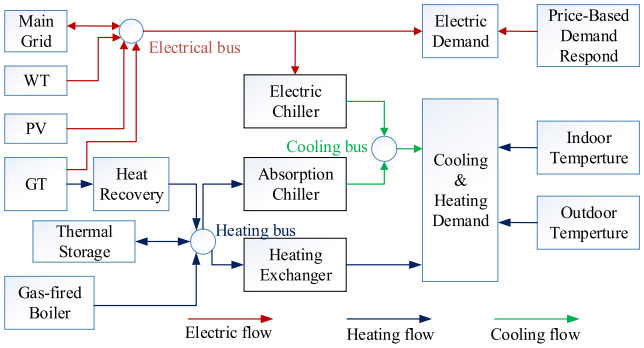

FIGURE 1. A framework of a multi-energy system.

management strategies and dispatch schemes need to be modified to better provide various energy to the end-users.

Multiple devices are required to achieve multiple energy conversion processes, including electric chillers, absorption chillers, heating exchangers, heat recovery systems, and thermal storage. As shown in Fig. 1, the electric demand of the end-users can be satisfied by the main grid and different distributed generations. The cooling demand can be provided by the electric chillers and absorption chillers. The heating demand can be provided by the gas-fired boilers, heat recovery systems, and thermal storage.

III. A TWO-STAGE COLLABORATIVE OPERATION STRATEGY OF A MULTI-ENERGY SYSTEM

In order to obtain an intra-day scheduling plan for a multi-energy system under consideration of multiple uncertainties, the collaborative scheduling optimization framework proposed in this paper contains both upper- and lower-level optimization models. The upper-level optimization model is a robust day-ahead scheduling plan; the lower-level optimization model is an intra-day rolling scheduling plan considering uncertainties at shorter time scales.

A. DAY-AHEAD ROBUST LINEAR SCHEDULING

1) ELECTRIC DEMAND-CONTROLLED STRATEGY

By setting proper real-time tariffs to enable the electric load shifting is also known as an electric demand-controlled strategy. The price-based demand response has been widely applied, and in this paper, a real time pricing model is developed to implement the demand response program [9]. The response model is shown as follows:

$$\begin{cases} \gamma_t = E_{0,t}/E_{\text{av}} \\ p_{\text{RTP},t} = \gamma_t \cdot p_{\text{ref}} \\ p_{\text{RTP}}^{\min} \le p_{\text{RTP},t} \le p_{\text{RTP}}^{\max} \end{cases} \tag{1}$$

$$E_{\text{EL},t} = E_{0,t} + \varepsilon E_{0,t}\left(p_{\text{RTP},t} - p_{\text{ref}}\right)/p_{\text{ref}} \tag{2}$$

where $E_{0,t}$ and E_{av} are the initial electricity demand at time t and average value of electric load in a day respectively; $p_{\text{RTP}}^{\min}$ and $p_{\text{RTP}}^{\max}$ are the lower and upper limits of the real time pricing. ε is the elasticity coefficient and according to the reference [16], the elasticity coefficient is set to be -0.3.

2) SCK-TYPE ROBUST LINEAR OPTIMIZATION

The typical robust linear optimization model is given as:

$$\begin{cases} \min\ \boldsymbol{c}^{\mathrm{T}}\boldsymbol{x} \\ \text{s.t. } \boldsymbol{A}\boldsymbol{x} \le \boldsymbol{b} \\ \quad \boldsymbol{l} \le \boldsymbol{x} \le \boldsymbol{u} \end{cases} \tag{3}$$

where $\boldsymbol{x}, \boldsymbol{u}, \boldsymbol{l} \in \mathbf{R}^{\text{n}}$ are the decision variable vector of the optimization model and their upper and lower budgets respectively; $\boldsymbol{c} \in \mathbf{R}^{\text{n}}$ is the vector of coefficients of the objective function of the optimization model. $\boldsymbol{A} \in \mathbf{R}^{\text{mn}}$, $\boldsymbol{b} \in \mathbf{R}^{\text{m}}$ are the constraint coefficient matrix and coefficient vector of the model, respectively. Assume that the random variables between any 2 inequality constraints are independent of each other and only the coefficient matrix $\boldsymbol{A}$ contains the random variable elements a_{ij} ($a_{ij} \in \left[a_{ik}^{\text{L}}, a_{ik}^{\text{U}}\right]$, $E(a_{ij}) \in \bar{a}_{ij}$).

Introducing the robust index $\Gamma_i (\Gamma_i \le |J_i|)$, which denotes the uncertainty measure of the i^{th} inequality constraint. J_i denotes the set of random variables in the i^{th} row of $\boldsymbol{A}$, and $|J_i|$ denotes the number of sets. The relationship between the $\boldsymbol{a}_i$ and Γ_i for i^{th} row containing random variables in $\boldsymbol{A}$ can be expressed as:

$$\begin{aligned} &\Re_i(\Gamma_i) \\ &= \left\{ \begin{array}{l} \boldsymbol{a}_i | a_{ik} \in \left[\bar{a}_{ik} - \beta_{ik}\left(\bar{a}_{ik} - a_{ik}^{\text{L}}\right), \bar{a}_{ik} + \beta_{ik}\left(a_{ik}^{\text{U}} - \bar{a}_{ik}\right)\right], \\ 0 \le \beta_{ik} \le 1, \sum\limits_{k \in J_i} \beta_{ik} \le \Gamma_i \end{array} \right\} \\ &\qquad\qquad i = 1, 2, \cdots, m, \quad \forall k \in J_i \end{aligned} \tag{4}$$

where β_{ik} denotes the weighting factor of the element a_{ik}. By introducing new decision variables z_i and p_{ik}, the typical robust linear model with uncertain variables can be transformed into an SCK-type robust linear model [26], as shown in the following:

$$\begin{cases} \min\ \boldsymbol{c}^{\mathrm{T}}\boldsymbol{x} \\ \text{s.t. } \sum\limits_{j=1}^{n} \bar{a}_{ij} + \Gamma_i z_i + \sum\limits_{k \in J_i} p_{ik} \le b_i, \quad i = 1, \cdots, m \\ \quad z_i + p_{ik} \ge \left(\bar{a}_{ik} - a_{ik}^{\text{L}}\right) \cdot x_k, \quad i = 1, \cdots, m, \ \forall k \in J_i \\ \quad z_i + p_{ik} \ge -\left(a_{ik}^{\text{U}} - \bar{a}_{ik}\right) \cdot x_k, \quad i = 1, \cdots, m, \ \forall k \in J_i \\ \quad z_i \ge 0, \quad p_{ik} \ge 0, \ i = 1, \cdots, m, \ \forall k \in J_i \\ \quad \boldsymbol{l} \le \boldsymbol{x} \le \boldsymbol{u} \end{cases} \tag{5}$$

3) DAY-AHEAD LINEAR ROBUST SCHEDULING MODEL

a: OBJECTIVE FUNCTION

$$\begin{aligned} &\min\ C^{\text{U}} \\ &= C_{\text{NG}} + C_{\text{grid}} + C_{\text{M}} \\ &= p_{\text{NG}} \sum_{t \in \text{T}} \frac{F_{\text{GB},t} + F_{\text{PGU},t}}{\sigma_{\text{LHV}}} + \sum_{t \in \text{T}} c_{\text{grid},t}^{\text{buy}} P_{\text{grid},t}^{\text{buy}} \tau - c_{\text{grid},t}^{\text{sell}} P_{\text{grid},t}^{\text{sell}} \tau \\ &\quad + \sum_{t \in \text{T}} c_{\text{GT}} P_{\text{GT},t} \tau + c_{\text{WT}} P_{\text{WT},t} \tau + c_{\text{PV}} P_{\text{PV},t} \tau \end{aligned} \tag{6}$$

where C^{U} is the daily operation cost which includes natural gas purchased cost C_{NG}, electric energy transaction cost C_{grid} and maintenance cost C_{M}; σ_{LHV} and p_{NG} are the low heat value and purchase price of natural gas respectively; c_{GT}, c_{WT} and c_{PV} are the maintenance cost per unit capacity of gas turbine, WT and PV respectively.

b: CONSTRAINTS

In the day-ahead scheduling stage, the constraints mainly include multi-energy balance constraints, energy purchase constraints, equipment operation constraints and price-based demand response constraints.

Constraints on multi-energy balance are as follows:

$$\begin{cases} P_{\mathrm{GT},t} + P_{\mathrm{PV},t} + P_{\mathrm{WT},t} + P_{\mathrm{grid},t} = P_{\mathrm{EC},t} + P_{\mathrm{EL},t} \\ Q_{\mathrm{CE},t} = Q_{\mathrm{EC},t} + Q_{\mathrm{AC},t} \\ Q_{\mathrm{HRS},t} + Q_{\mathrm{GB},t} - Q_{\mathrm{TSC},t} + Q_{\mathrm{TSD},t} \\ \qquad = Q_{\mathrm{RC},t} + Q_{\mathrm{RH},t} + Q_{\mathrm{waste},t} \end{cases} \tag{7}$$

where $P_{\mathrm{GT},t}$, $P_{\mathrm{PV},t}$ and $P_{\mathrm{WT},t}$ are the power output of gas turbines, PV and WT at time t respectively; $P_{\mathrm{grid},t}$, $P_{\mathrm{EC},t}$ and $P_{\mathrm{EL},t}$ are the electric power exchanging from grid, electric power consumed by electric chillers and electric power load at time t respectively. $Q_{\mathrm{CE},t}$ is cooling load; $Q_{\mathrm{EC},t}$ and $Q_{\mathrm{AC},t}$ are the cooling energy output power of electric chillers and absorption chillers at time t respectively; $Q_{\mathrm{HRS},t}$ and $Q_{\mathrm{GB},t}$ are the thermal energy recovered from the gas turbine and provided from the gas-fired boiler at time t respectively; $Q_{\mathrm{TSC},t}$ and $Q_{\mathrm{TSD},t}$ are the heat charging and discharging of the thermal storage at time t respectively; $Q_{\mathrm{RC},t}$ and $Q_{\mathrm{RH},t}$ are the total thermal energy recovered for cooling and heating at time t respectively.

Constraints on equipment operation are as follows:

$$\begin{cases} 0 \le P_{\mathrm{GT},t} \le u_{\mathrm{GT},t} P_{\mathrm{GT}}^{\max} \\ -r_{\mathrm{GT}} P_{\mathrm{GT}}^{\max} \le P_{\mathrm{GT},t} - P_{\mathrm{GT},t-1} \le r_{\mathrm{GT}} P_{\mathrm{GT}}^{\max} \\ 0 \le P_{\mathrm{PV},t} \le P_{\mathrm{PV}}^{\max} \\ 0 \le P_{\mathrm{WT},t} \le P_{\mathrm{WT}}^{\max} \\ 0 \le Q_{\mathrm{GB},t} \le Q_{\mathrm{GB}}^{\max} \\ 0 \le Q_{\mathrm{EC},t} \le Q_{\mathrm{EC}}^{\max} \\ 0 \le Q_{\mathrm{AC},t} \le Q_{\mathrm{AC}}^{\max} \\ 0 \le Q_{\mathrm{HE},t} \le Q_{\mathrm{HE}}^{\max} \end{cases} \tag{8}$$

$$\begin{cases} Q_{\mathrm{TS},t} = \eta_{\mathrm{TS}} Q_{\mathrm{TS},t-1} + \eta_{\mathrm{TSC}} Q_{\mathrm{TSC},t} - Q_{\mathrm{TSD},t}/\eta_{\mathrm{TSD}} \\ \alpha_{\mathrm{TSC},t} + \alpha_{\mathrm{TSD},t} \le 1 \\ 0 \le Q_{\mathrm{TSC},t} \le \alpha_{\mathrm{TSC},t} Q_{\mathrm{TSC},t}^{\max} \\ 0 \le Q_{\mathrm{TSD},t} \le \alpha_{\mathrm{TSD},t} Q_{\mathrm{TSD}}^{\max} \\ Q_{\mathrm{TS}}^{\min} \le Q_{\mathrm{TS},t} \le Q_{\mathrm{TS}}^{\max} \\ Q_{\mathrm{TS},0} = Q_{\mathrm{TS},24} \end{cases} \tag{9}$$

where $P_{\mathrm{GT}}^{\max}$, $P_{\mathrm{PV}}^{\max}$, $P_{\mathrm{WT}}^{\max}$, $Q_{\mathrm{GB}}^{\max}$, $Q_{\mathrm{EC}}^{\max}$, $Q_{\mathrm{AC}}^{\max}$ and $Q_{\mathrm{HE}}^{\max}$ are the nominal capacity of the corresponding energy equipment in the multi-energy system. r_{GT} is the ramping rate of the gas turbine. $Q_{\mathrm{TS},t}$ represents the thermal energy storage state at time t; $Q_{\mathrm{TSC},t}$ and $Q_{\mathrm{TSD},t}$ are the heat charging and discharging of the thermal storage at time t respectively; $Q_{\mathrm{TS}}^{\max}$ and $Q_{\mathrm{TS}}^{\min}$ represent the minimal and maximal limits of the thermal energy storage state; $u_{\mathrm{GT},t}$, $\alpha_{\mathrm{TSC},t}$ and $\alpha_{\mathrm{TSD},t}$ are binary operation variables of the gas turbine and thermal energy storage.

Constraints on energy interaction are as follows:

$$\begin{cases} -P_{\mathrm{grid}}^{\max} \le P_{\mathrm{grid},t} \le P_{\mathrm{grid}}^{\max} \\ 0 \le F_{\mathrm{NG},t} \le F_{\mathrm{NG}}^{\max} \end{cases} \tag{10}$$

where $P_{\mathrm{grid}}^{\max}$ and $F_{\mathrm{NG}}^{\max}$ are the upper limits of electricity exchange and purchase of natural gas.

Constraints on random variables are as follows:

$$\begin{cases} P_{\mathrm{WT},t} = \bar{P}_{\mathrm{WT},t} + \hat{P}_{\mathrm{WT},t} \\ \hat{P}_{\mathrm{WT},t}^{\mathrm{L}} \le \hat{P}_{\mathrm{WT},t} \le \hat{P}_{\mathrm{WT},t}^{\mathrm{U}} \\ P_{\mathrm{PV},t} = \bar{P}_{\mathrm{PV},t} + \hat{P}_{\mathrm{PV},t} \\ \hat{P}_{\mathrm{PV},t}^{\mathrm{L}} \le \hat{P}_{\mathrm{PV},t} \le \hat{P}_{\mathrm{PV},t}^{\mathrm{U}} \end{cases} \tag{11}$$

where $\bar{P}_{\mathrm{WT},t}$ and $\bar{P}_{\mathrm{PV},t}$ are the predicted power output of WT and PV at time t respectively; $\hat{P}_{\mathrm{WT},t}$ and $\hat{P}_{\mathrm{PV},t}$ are the fluctuating value of WT and PV power output at time t respectively; $\hat{P}_{\mathrm{WT},t}^{\mathrm{U}}$, $\hat{P}_{\mathrm{PV},t}^{\mathrm{U}}$, $\hat{P}_{\mathrm{WT},t}^{\mathrm{L}}$ and $\hat{P}_{\mathrm{PV},t}^{\mathrm{L}}$ are the upper and lower limits of the fluctuation value of the corresponding output power.

4) LINEARIZATION TRANSFORMATION

For the inequality constraint with random variables in the mathematical model, a robust equivalent linear transformation of (11) is conducted according to the linear optimization theory [26]. Taking the uncertain variable as PV power generation as an example, the robust equivalent linear transformation is conducted concerning the transformation (5), and the results are as follows:

$$\begin{cases} \bar{P}_{\mathrm{PV},t} - P_{\mathrm{PV}}^{\max} + \Gamma z_{\mathrm{PV},t} + \sum_{t \in \mathrm{T}} p_{\mathrm{PV},t} \le 0 \\ z_{\mathrm{PV},t} + p_{\mathrm{PV},t} \ge \hat{P}_{\mathrm{PV},t}^{\mathrm{U}} \\ z_{\mathrm{PV},t} + p_{\mathrm{PV},t} \ge \hat{P}_{\mathrm{PV},t}^{\mathrm{L}} \\ z_{\mathrm{PV},t} \ge 0, \quad p_{\mathrm{PV},t} \ge 0 \end{cases} \tag{12}$$

where $z_{\mathrm{PV},t}$ and $p_{\mathrm{PV},t}$ are the newly introduced decision variables in the robust equivalent linear transformation process.

B. INTRA-DAY ROLLING STOCHASTIC SCHEDULING

1) THERMAL DEMAND-CONTROLLED STRATEGY

By setting an appropriate indoor temperature value in the comfort temperature range can realize the thermal demand-controlled strategy.

In this paper, only the temperature-dependent thermal loads are taken into consideration. To be specific, these cooling and heating loads of the buildings are dependent on the indoor temperature set value and outdoor temperature. As there is a certain range of the thermal comfort temperature, the thermal loads are flexible in a corresponding range [13]. The differential equation of heat balance of the building

envelope can be shown as:

$$p_{\mathrm{HE}} - p_{\mathrm{CE}} = \rho V C \frac{dT_{\mathrm{in},t}}{dt} - \left(k_{\mathrm{wall}} S_{\mathrm{wall}} + k_{\mathrm{win}} S_{\mathrm{win}}\right) \times \left(T_{\mathrm{out},t} - T_{\mathrm{in},t}\right) - G k_{\mathrm{c}} S_{\mathrm{win}} \quad (13)$$

where p_{HE} and p_{CE} are the heating and cooling energy injected into the building respectively; and these two variables cannot exist at the same time. $T_{\mathrm{out},t}$ and $T_{\mathrm{in},t}$ are the outdoor and indoor temperature at time t. ρ, V and C are the air density, air specific heat capacity and air volume, respectively; k_{wall} and k_{win} are shading coefficient of the wall and the window of the building, respectively; S_{wall} and S_{win} are wall and window area, respectively; G is the solar radiation.

To discretize the above equation, the cooling energy and heating energy demand can be calculated as:

$$Q_{\mathrm{CE},t} = \begin{cases} \left(k_{\mathrm{wall}} S_{\mathrm{wall}} + k_{\mathrm{win}} S_{\mathrm{win}}\right)\left(T_{\mathrm{out},t} - T_{\mathrm{in},t}\right) + G_t k_{\mathrm{c}} S_{\mathrm{win}} \\ \quad - \rho V C \left(T_{\mathrm{in},t} - T_{\mathrm{in},t-1}\right)/\tau & T_{\mathrm{out},t} > T_{\mathrm{in}}^{\max} \\ 0 & T_{\mathrm{out},t} \le T_{\mathrm{in}}^{\min} \end{cases} \quad (14)$$

$$Q_{\mathrm{HE},t} = \begin{cases} \rho V C \left(T_{\mathrm{in},t} - T_{\mathrm{in},t-1}\right)/\tau - G_t k_{\mathrm{c}} S_{\mathrm{win}} \\ \quad - \left(k_{\mathrm{wall}} S_{\mathrm{wall}} + k_{\mathrm{win}} S_{\mathrm{win}}\right)\left(T_{\mathrm{out},t} - T_{\mathrm{in},t}\right) \\ \quad T_{\mathrm{out},t} \le T_{\mathrm{in}}^{\min} \\ 0 \quad T_{\mathrm{out},t} > T_{\mathrm{in}}^{\max} \end{cases} \quad (15)$$

where $T_{\mathrm{in}}^{\min}$ and $T_{\mathrm{in}}^{\max}$ are the minimum and maximum indoor temperature. The constraint of the changing rate limit of the indoor temperature can be shown as:

$$r_{\mathrm{in}}^{\min} \le T_{\mathrm{in},t} - T_{\mathrm{in},t-1} \le r_{\mathrm{in}}^{\max} \quad (16)$$

2) STOCHASTIC UNCERTAINTY OF DG AND ELECTRIC LOADS

Renewable energy output and electric energy demand forecasts generally become more accurate as the forecast time scale is reduced. In intraday scheduling stage, the normal distribution is applied to model the intraday prediction errors of PV and WT outputs and electric load.

$$\begin{cases} f\left(\xi_{\mathrm{WT}}\right) = \dfrac{1}{\sigma_{\mathrm{WT}}\sqrt{2\pi}} e^{-\left(\xi_{\mathrm{WT}} - \mu_{\mathrm{WT}}\right)^2 / 2\sigma_{\mathrm{WT}}^2} \\ f\left(\xi_{\mathrm{PV}}\right) = \dfrac{1}{\sigma_{\mathrm{PV}}\sqrt{2\pi}} e^{-\xi_{\mathrm{PV}}^2 / 2\sigma_{\mathrm{PV}}^2} \\ f\left(\xi_{\mathrm{EL}}\right) = \dfrac{1}{\sigma_{\mathrm{EL}}\sqrt{2\pi}} e^{-\xi_{\mathrm{EL}}^2 / 2\sigma_{\mathrm{EL}}^2} \end{cases} \quad (17)$$

where ξ_{WT}, ξ_{PV} and ξ_{EL} denote the intraday power deviations of PV outputs, WT outputs and electric load respectively; μ_{WT}, σ_{WT}, σ_{PV} and σ_{EL} represent the corresponding distribution coefficients. The method of Latin Hypercube Sampling is applied to generate the initial scenarios of PV output, WT output and electric load. Moreover, the method of simultaneous backward reduction is used to realize the process of scenarios reduction.

3) INTRA-DAY ROLLING STOCHASTIC SCHEDULING MODEL

a: OBJECTIVE FUNCTION

$$\begin{aligned} \min\ C^{\mathrm{L}} &= C_{\mathrm{NG}} + C_{\mathrm{grid}} + C_{\mathrm{M}} + C_{\mathrm{pen}} \\ &= p_{\mathrm{NG}} \sum_{t=t_r}^{N_r} \frac{F_{\mathrm{GB},t} + F_{\mathrm{PGU},t}}{\sigma_{\mathrm{LHV}}} \\ &\quad + \sum_{t=t_r}^{N_r} c_{\mathrm{grid},t}^{\mathrm{buy}} P_{\mathrm{grid},t}^{\mathrm{buy}} \tau - c_{\mathrm{grid},t}^{\mathrm{sell}} P_{\mathrm{grid},t}^{\mathrm{sell}} \tau \\ &\quad + \sum_{t=t_r}^{N_r} c_{\mathrm{GT}} P_{\mathrm{GT},t} \tau + c_{\mathrm{WT}} P_{\mathrm{WT},t} \tau + c_{\mathrm{PV}} P_{\mathrm{PV},t} \tau \\ &\quad + \sum_{t=t_r}^{N_r} c_{\mathrm{pen}} \left| T_{\mathrm{in},t} - T_{\mathrm{set}} \right| \end{aligned} \quad (18)$$

where t_r is the starting period of rolling optimization and N_r is the total number of periods in a rolling cycle. C_{pen} is the comfortable temperature penalty fee.

b: CONSTRAINTS

In the intraday rolling scheduling stage, considering the strong inertia of the thermal load, all equipment give response within 1 hour. The constraints include formula (7)-(10), (14)-(17).

4) MODEL SOLVING

Both day-ahead and intraday optimal scheduling model are mixed integer linear programming (MILP) problems, which can be formulated in Matlab and solved by a commercial solver Gorubi. The flow chart of model solving is shown in Fig. 2.

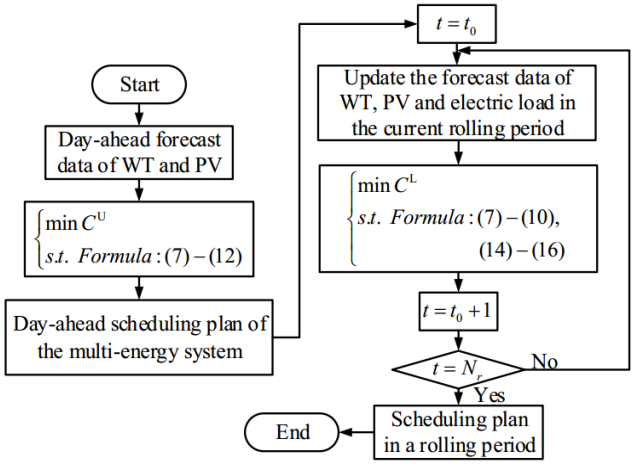

FIGURE 2. Flow chart of model solving.

IV. CASE STUDY

A. SYSTEM DESCRIPTION

To verify the effectiveness of the proposed collaborative interaction strategy, a multi-energy system is given in Beijing, China to provide different types of energy to a

residential zone. Table 6 (in Appendix A) shows the technical parameters of the multi-energy system and Table 7 (in Appendix A) shows the energy price of the multi-energy system. Table 8 (in Appendix A) shows the technical parameters of the residential zone. Figure 5 (in Appendix B) shows the interval predictions of PV power outputs, WT power outputs, electric loads and the outdoor temperature in a typical clear-sky day in autumn.

B. RESULTS AND AYALYSIS

1) ANALYSIS OF DAY-AHEAD SCHEDULING RESULTS

The day-ahead scheduling results can be obtained by solving the upper-level optimization model. The computation time to solve the upper-level model using the solver Gurobi is very short, only 2.3 seconds.

The energy supply and demand schedule results are shown in Fig. 3 and we can clearly find that with this robust linear optimization method in the first stage scheduling, the multi-energy system can fully achieve the balance of multiple energy sources while meeting the multiple energy demands on the user side. A detailed analysis of the multiple energy flowing is carried out, based on energy prices.

In Fig. 3(a), due to the low partial load rate of the gas turbine and the low cost of purchasing electricity from the grid, the electrical load of the end-users area is met by the electricity generated by the WT together with the electricity transmitted from the upper grid during the time period 22:00 to 7:00. As the cost of purchasing electricity from the upper grid rises, the proportion of electricity generated by gas turbines is higher than the amount of electricity purchased from the upper grid during the 8:00 to 21:00 time period.

During this time period, the distributed generating units also supply electricity to end users. In Fig. 3(b), during the period from 8:00 to 18:00, absorption chillers and electric chillers work during this time period to provide cold energy to end users because the outdoor temperature is above the upper limit of human comfort temperature range. In Fig. 3(c), the heat load for room heating exists during the timeperiod 19:00 to 7:00. During the time period 19:00 to 24:00, the heat load is mainly provided by the residual heat recovered by the gas turbine together with the gas-fired boilers. Since the gas turbine stops working during the 1:00-7:00 time period, the gas-fired boiler and the thermal storage tank provide the heat demand of the end-users at the same time.

2) ANALYSIS OF INTRA-DAY ROLLING STOCHASTIC SCHEDULING RESULTS

The intra-day rolling scheduling results can be obtained by solving the lower-level optimization model. The computation time to solve the lower -level model using the commercial solver Gurobi is also fast, taking only 4.3 seconds.

The energy supply and demand scheduling results of the intraday rolling schedule are shown in Fig. 4 and we can clearly find that in the second stage scheduling, the multi-energy system can fully achieve the balance of

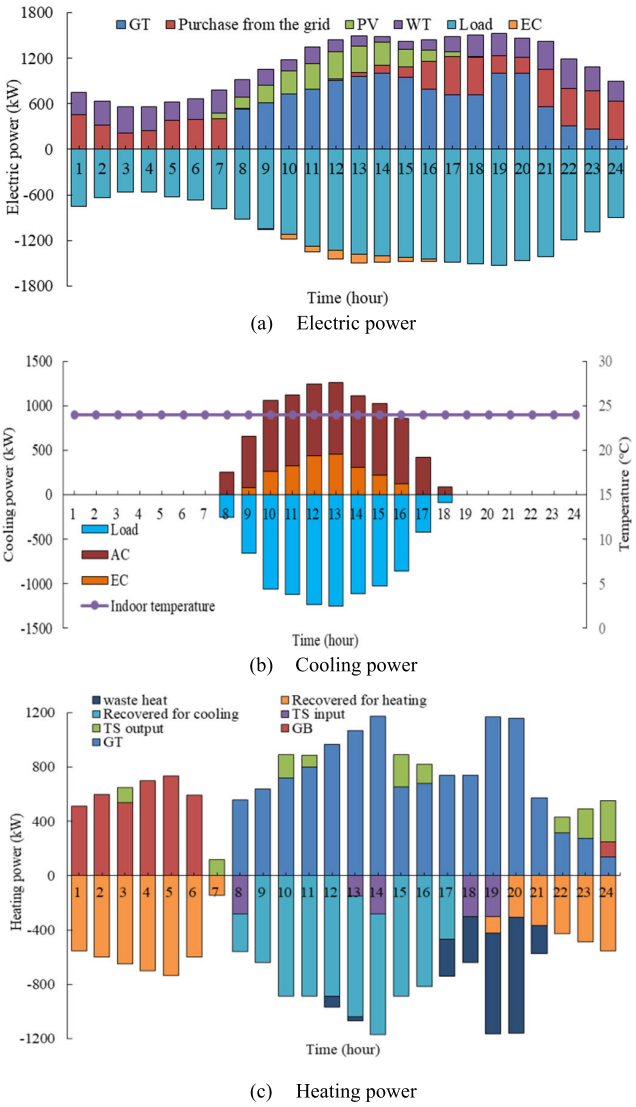

(a) Electric power

(b) Cooling power

(c) Heating power

FIGURE 3. Results of energy supply and demand scheduling in the day-ahead stage.

multiple energy sources while meeting the multiple energy demands on the user side. However, there are differences in the specific details of the day-ahead and intraday scheduling plans, which are caused by the fact that the intra-day forecast is more accurate than the day-ahead forecast.

Moreover, the control of flexible thermal load which can further cope with the uncertainty of intra-day scenic power generation while satisfying the end-user's body temperature comfort range, allows the system to operate under the most economical way. In Fig. 4(b), taking into account energy prices and indoor temperature setting value, the total cold energy demand of end-users in the intra-day dispatch plan is lower from 8:00 to 16:00 than the total cold energy demand in the day-ahead dispatch plan. However, from 17:00 to 19:00, the total amount of cold energy demanded by end-users in the intraday scheduling plan is higher. In Fig. 4(c), the amount of thermal energy used to heat the rooms in the intra-day

TABLE 1. The operation cost in different scheduling stages.

Scheduling stage	Operation cost ($)	Maintenance cost ($)	Electricity purchased cost ($)	Gas purchased cost ($)	Comfort penalty cost ($)
Day-ahead	2605.4	188.1	613.6	1803.7	-
Rolling	2556.5	186.6	581.5	1732.1	56.2

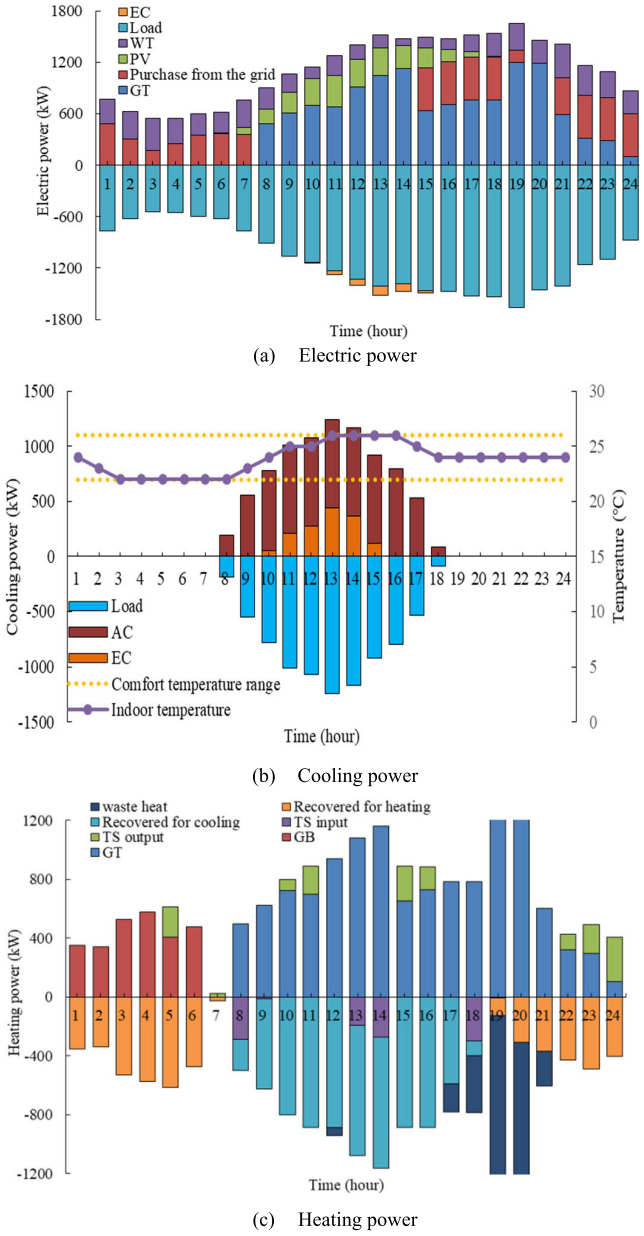

(a) Electric power

(b) Cooling power

(c) Heating power

FIGURE 4. Results of energy supply and demand scheduling in the intra-day rolling stage.

scheduling plan was lower than the amount in the day-ahead scheduling in every period, except at the moment 23:00, in which the total thermal demand increased by 107 kWh.

Furthermore, the results of operation cost and its item cost of the multi-energy system in two different scheduling stage are shown in Tab. 1. It is clearly found that all costs in the intra-day rolling optimization stage are lower than those in the day-ahead scheduling plan. This is due to the decreased uncertainty in the source-load imbalance power predicted during the day. In addition, the flexible heating and cooling loads are managed in the rolling stage, and the entire multi-energy system is dynamically optimized without impairing end-user temperature comfort and while satisfying multiple energy balances.

3) MUTIPLE ENERGY DEMAND-CONTROLLED ANALYSIS

Noting that electric energy demand-controlled for flexible electric loads in day-ahead scheduling stage and thermal energy demand-controlled for flexible thermal loads in intra-day rolling scheduling stage play a vital role in optimal operation of the multi-energy system. Three scenarios are carried out to analyze the positive effects of those two strategies of flexible electric and thermal loads. The detailed scenarios classifications are shown in table 2.

TABLE 2. The scenarios classification.

Scenarios	Flexible electric load	Flexible thermal load
1	√	√
2	√	
3		√

The simulation results for the three scenarios are shown in Tab. 3. Two indicators, primary energy consumption and carbon emissions, are also included in these analyses. As can be seen from Tab. 3, when the flexible electrical load and the flexible thermal load are not controlled, the total operating cost increases by 1.8% and 3.2%, respectively. The management of flexible electrical and thermal loads in day-ahead stage and intra-day stage offers strong potential for more economical, environmental and optimal operation of the multi-energy system. This is because in day-ahead stage, the partial load in peak periods can be shifted by the management of flexible electric loads. Moreover, the management of flexible thermal loads is essentially the incorporation of virtual energy storage technology into the intra-day rolling stage. Consequently, a proper control of the flexible loads in different scheduling stage can effectively relieve the energy supply pressure and can reduce primary energy consumption as well as reduce carbon emissions.

4) COMPARISON OF EFFECTIVENESS OF DIFFERENT OPTIMIZATION METHODS

This section compares the effectiveness of the proposed optimization method with the existing optimization method

TABLE 3. The operation cost with different robustness factors.

Scenarios	Total operation cost ($)	Increased	Primary energy consumption (kWh)	Increased	Carbon emissions (kg)	Increased
1	2556.5	-	58922	-	13924	-
2	2637.4	3.2%	62850	6.7%	14813	6.4%
3	2602.5	1.8%	60159	2.1%	14313	2.8%

for day-ahead economic scheduling and intra-day economic scheduling.

In the first stage optimization model, the proposed robust linear optimization (Method A) and other two methods: the typical robust optimization (Method B) and the stochastic optimization (Method C). When using method A and method B, the robustness factor is set to be 1. When using method C, 1000 scenarios were simulated by using the Latin Hypercube Sampling method for WT and PV output and electric load, respectively. These scenarios are then reduced to 5 typical scenarios using the k-means clustering approach.

The comparison results are shown in Table 4. Considering the same robustness factor, the operation costs after the optimization using Method A and Method B are very similar and both are roughly $100 higher than the operation cost optimized by method C. This is due to the conservative nature of robust optimization. However, it is obvious that with the proposed robust linear optimization model, the computation time of the optimization process is significantly lower than that of Method B and Method C. The results of operation cost and the computation time verify the proposed method has significant robustness to achieve the balance of multiple energy sources, as well as the advantage of computational speed in a model for the day-ahead scheduling.

TABLE 4. Comparison results in first-stage model.

Method	A (proposed)	B	C
Operation cost ($)	2605.4	2616.1	2515.2
Computation time (s)	2.3	2.9	3.8

In the second stage optimization model, the proposed rolling stochastic optimization (Method D) and other two methods: rolling optimization (Method E) and stochastic optimization (Method F). When using method D and method E, the control time window is set to 1 hour. When using method D and method F, the optimization process uses the same set of typical scenarios.

The comparison results are shown in Table 5. Comparing the three methods, the proposed method in this paper can ensure that the system has the lowest operation cost under multiple uncertainties considering shorter time scales in a day. It also proves that the control of flexible electric and thermal loads can effectively improve the overall energy efficiency and reduce operating costs. In terms of temperature comfort rate, the proposed method can maintain system stability without harming end-user comfort benefits. However, the proposed approach is not as fast as Method E and Method F in terms of computational speed, but this computational time is affordable. The results of operation cost, temperature comfort rate and computation time can verify the proposed rolling stochastic optimization method can guarantee the stable operation of the system without impairing the indoor temperature comfort of the end-users as well as guaranteeing the economy of the system.

TABLE 5. Comparison results in second-stage model.

Method	D (proposed)	E	F
Operation cost ($)	2556.5	2834.3	2784.9
Temp. comfort rate (%)	100%	87.2%	78.9%
Computation time (s)	4.3	3.8	3.5

V. CONCLUSION

A novel optimal operation strategy is proposed for a multi-energy system based on the multiple energy demand-controlled solution for flexible electric and thermal loads in different time scales. The robust linear optimization method is applied in the day-ahead scheduling stage and the rolling stochastic approach is used in the intra-day scheduling stage. Several case studies are carried out to prove the effectiveness and advantages of the proposed method and several meaningful conclusions can be drawn as follows:

- The proposed collaborative operation strategy can achieve a coordinated operation of a multi-energy system in both day-ahead and intra-day stages as well as ensuring a balance between supply and demand of multiple energy sources with the consideration of the multiple uncertainties of wind power, solar power and electric loads;
- The multiple energy demand-controlled solution for flexible electric and thermal loads can realize the load shifting in the day-ahead scheduling stage and create flexibility in energy demand to cope with the fluctuations in renewable power output and electric load in the intra-day scheduling stage;
- With the proposed model in this paper, not only the stable and reliable operation of the multi-energy system can be effectively achieved, but also the three indexes of economy, energy and environment can be improved during the operation process. Moreover, the proposed strategy is easy to implement and it has high engineering practicality.

APPENDIX A

Appendix A shows three tables of technical parameters of multi-energy system, energy price in multi-energy system and technical parameters of residential zone.

TABLE 6. Technical parameters of multi-energy system.

Parameter	Unit	Value	Parameter	Unit	Value
P_{GT}^{max}	kW	1000	η_{GB}	%	90
Q_{TS}^{max}	kWh	800	η_{AC}	-	0.7
Q_{TS}^{min}	kWh	200	η_{EC}	-	4
Q_{TSC}^{max}	kWh	150	η_{TSC}	%	95
Q_{TSD}^{max}	kWh	150	η_{TSD}	%	95
Q_{GB}^{max}	kWh	800	r_{GT}	%	50
Q_{EC}^{max}	kWh	800	c_{GT}	\$/kWh	0.008
Q_{AC}^{max}	kWh	800	c_{WT}	\$/kWh	0.010
P_{grid}^{max}	kW	500	c_{PV}	\$/kWh	0.012
η_{GT}	%	35	τ	h	1
η_{loss}	%	15	σ_{LHV}	kWh/m^3	9.78
η_{HRS}	%	80	p_{RTP}^{max}	\$	0.250
η_{HE}	%	80	p_{RTP}^{min}	\$	0.045

TABLE 7. Energy price in multi-energy system.

Parameter	Time period	Value	Parameter	Time period	Value
$c_{grid,t}^{buy}$	Peak [a]	0.235	p_{ref}	Peak	0.178
(\$/kWh)	Flat [b]	0.129	(\$/kWh)	Flat	0.133
	Valley [c]	0.051		Valley	0.073
$c_{grid,t}^{sell}$	Peak	0.207	p_{NG}	Whole day	0.45
(\$/kWh)	Flat	0.129	(\$/m^3)		
	Valley	0.055			

[a] Peak: 14:00–16:59, 19:00–21:59;
[b] Flat: 8:00–13:59, 17:00–18:59, 22:00–23:59;
[c] Valley: 0:00-7:59.

TABLE 8. Technical parameters of residential zone.

Parameter	Unit	Value	Parameter	Unit	Value
ρ	kg/m^3	1.293	S_{win}	m^2	400
V	m^3	3.06×10^6	k_{sh}	-	0.45
k_{win}	W(m^2□K)$^{-1}$	2.7	T_{in}^{max}	℃	20
k_{wall}	W(m^2□K)$^{-1}$	0.92	T_{in}^{min}	℃	24
S_{wall}	m^2	4200	$r_{in}^{max/min}$	℃	1

APPENDIX B

Appendix B shows the figures of day-ahead interval prediction profiles.

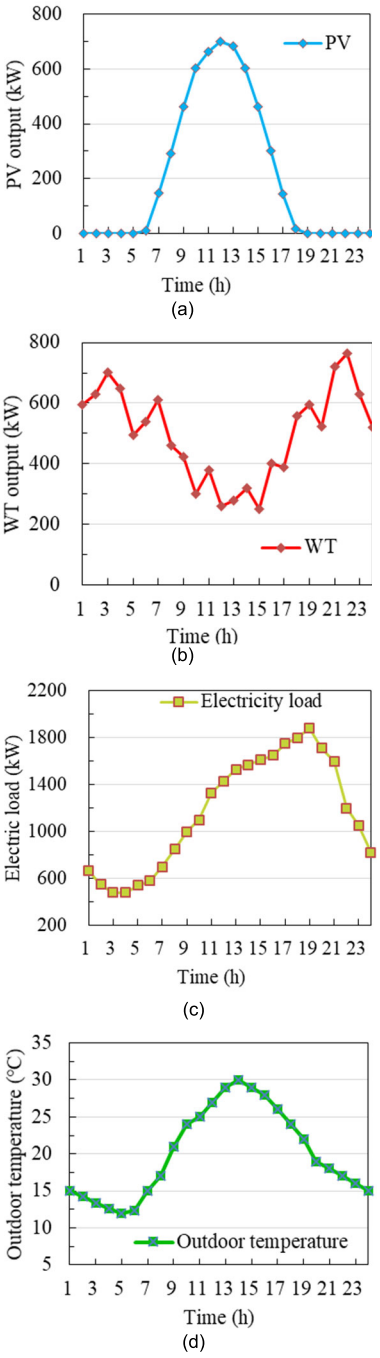

FIGURE 5. Day-ahead interval prediction profiles: (a) PV; (b) WT; (c) electric load; (d) outdoor temperature.

REFERENCES

[1] W. Gu, Z. Wu, R. Bo, W. Liu, G. Zhou, W. Chen, and Z. Wu, "Modeling, planning and optimal energy management of combined cooling, heating and power microgrid: A review," *Int. J. Electr. Power Energy Syst.*, vol. 54, pp. 26–37, Jan. 2014, doi: 10.1016/j.ijepes.2013.06.028.

[2] C. Klemm and P. Vennemann, "Modeling and optimization of multi-energy systems in mixed-use districts: A review of existing methods and approaches," *Renew. Sustain. Energy Rev.*, vol. 135, Jan. 2021, Art. no. 110206, doi: 10.1016/j.rser.2020.110206.

[3] S. M. Nosratabadi, R.-A. Hooshmand, and E. Gholipour, "A comprehensive review on microgrid and virtual power plant concepts employed for distributed energy resources scheduling in power systems," *Renew. Sustain. Energy Rev.*, vol. 67, pp. 341–363, Jan. 2017, doi: 10.1016/j.rser.2016.09.025.
[4] Y. Mao, J. Wu, and W. Zhang, "An effective operation strategy for CCHP system integrated with photovoltaic/thermal panels and thermal energy storage," *Energies*, vol. 13, no. 23, p. 6418, Dec. 2020, doi: 10.3390/en13236418.
[5] C. Lingmin, W. Jiekang, W. Fan, T. Huiling, L. Changjie, and X. Yan, "Energy flow optimization method for multi-energy system oriented to combined cooling, heating and power," *Energy*, vol. 211, Nov. 2020, Art. no. 118536, doi: 10.1016/j.energy.2020.118536.
[6] G. Yang and X. Q. Zhai, "Optimal design and performance analysis of solar hybrid CCHP system considering influence of building type and climate condition," *Energy*, vol. 174, pp. 647–663, May 2019, doi: 10.1016/j.energy.2019.03.001.
[7] W. Liu, G. Chen, B. Yan, Z. Zhou, H. Du, and J. Zuo, "Hourly operation strategy of a CCHP system with GSHP and thermal energy storage (TES) under variable loads: A case study," *Energy Buildings*, vol. 93, pp. 143–153, Apr. 2015, doi: 10.1016/j.enbuild.2015.02.030.
[8] Q. Wang, J. Liu, Y. Hu, and X. Zhang, "Optimal operation strategy of multi-energy complementary distributed CCHP system and its application on commercial building," *IEEE Access*, vol. 7, pp. 127839–127849, Sep. 2019, doi: 10.1109/access.2019.2939913.
[9] T. Ma, J. Wu, and L. Hao, "Energy flow modeling and optimal operation analysis of the micro energy grid based on energy hub," *Energy Convers. Manage.*, vol. 133, pp. 292–306, Feb. 2017, doi: 10.1016/j.enconman.2016.12.011.
[10] W. Yanan, W. Jiekang, and M. Xiaoming, "Intelligent scheduling optimization of seasonal CCHP system using rolling horizon hybrid optimization algorithm and matrix model framework," *IEEE Access*, vol. 6, pp. 75132–75142, 2018, doi: 10.1109/access.2018.2878044.
[11] Y. Huang, P. Ding, Y. Wang, S. Li, K. Yang, and Y. Li, "A bilevel optimal operation model of multi energy carriers system considering part load rate and demand response," *Sustain. Energy Technol. Assessments*, vol. 45, Jun. 2021, Art. no. 101035, doi: 10.1016/j.seta.2021.101035.
[12] R. Bahmani, H. Karimi, and S. Jadid, "Cooperative energy management of multi-energy hub systems considering demand response programs and ice storage," *Int. J. Electr. Power Energy Syst.*, vol. 130, Sep. 2021, Art. no. 106904, doi: 10.1016/j.ijepes.2021.106904.
[13] M. Sedighizadeh, M. Esmaili, and N. Mohammadkhani, "Stochastic multi-objective energy management in residential microgrids with combined cooling, heating, and power units considering battery energy storage systems and plug-in hybrid electric vehicles," *J. Cleaner Prod.*, vol. 195, pp. 301–317, Sep. 2018, doi: 10.1016/j.jclepro.2018.05.103.
[14] S. A. Mansouri, A. Ahmarinejad, M. S. Javadi, and J. P. S. Catalão, "Two-stage stochastic framework for energy hubs planning considering demand response programs," *Energy*, vol. 206, Sep. 2020, Art. no. 118124, doi: 10.1016/j.energy.2020.118124.
[15] Y. Zhou, W. Yu, S. Zhu, B. Yang, and J. He, "Distributionally robust chance-constrained energy management of an integrated retailer in the multi-energy market," *Appl. Energy*, vol. 286, Mar. 2021, Art. no. 116516, doi: 10.1016/j.apenergy.2021.116516.
[16] W. Hou, Z. Liu, L. Ma, and L. Wang, "A real-time rolling horizon chance constrained optimization model for energy hub scheduling," *Sustain. Cities Soc.*, vol. 62, Nov. 2020, Art. no. 102417, doi: 10.1016/j.scs.2020.102417.
[17] J. Zhou, Y. Wu, C. Wu, Z. Deng, C. Xu, and Y. Hu, "A hybrid fuzzy multi-criteria decision-making approach for performance analysis and evaluation of park-level integrated energy system," *Energy Convers. Manage.*, vol. 201, Dec. 2019, Art. no. 112134, doi: 10.1016/j.enconman.2019.112134.
[18] Z. Luo, W. Gu, Z. Wu, Z. Wang, and Y. Tang, "A robust optimization method for energy management of CCHP microgrid," *J. Modern Power Syst. Clean Energy*, vol. 6, no. 1, pp. 132–144, Jun. 2017, doi: 10.1007/s40565-017-0290-3.
[19] T. Zhang, M. Wang, P. Wang, J. Gu, W. Zheng, and Y. Dong, "Bi-stage stochastic model for optimal capacity and electric cooling ratio of CCHPs—A case study for a hotel," *Energy Buildings*, vol. 194, pp. 113–122, Jul. 2019, doi: 10.1016/j.enbuild.2019.04.004.
[20] V. C. Onishi, C. H. Antunes, E. S. Fraga, and H. Cabezas, "Stochastic optimization of trigeneration systems for decision-making under long-term uncertainty in energy demands and prices," *Energy*, vol. 175, pp. 781–797, May 2019, doi: 10.1016/j.energy.2019.03.095.
[21] C. Zhang, Y. Xu, Z. Li, and Z. Y. Dong, "Robustly coordinated operation of a multi-energy microgrid with flexible electric and thermal loads," *IEEE Trans. Smart Grid*, vol. 10, no. 3, pp. 2765–2775, May 2019, doi: 10.1109/tsg.2018.2810247.
[22] C. Zhang, Y. Xu, and Z. Y. Dong, "Robustly coordinated operation of a multi-energy micro-grid in grid-connected and islanded modes under uncertainties," *IEEE Trans. Sustain. Energy*, vol. 11, no. 2, pp. 640–651, Apr. 2020, doi: 10.1109/tste.2019.2900082.
[23] Z. Zhao, W. C. Lee, Y. Shin, and K.-B. Song, "An optimal power scheduling method for demand response in home energy management system," *IEEE Trans. Smart Grid*, vol. 4, no. 3, pp. 1391–1400, Sep. 2013, doi: 10.1109/tsg.2013.2251018.
[24] J. Wang, H. Zhong, Z. Ma, Q. Xia, and C. Kang, "Review and prospect of integrated demand response in the multi-energy system," *Appl. Energy*, vol. 202, pp. 772–782, Sep. 2017, doi: 10.1016/j.apenergy.2017.05.150.
[25] F. Brahman, M. Honarmand, and S. Jadid, "Optimal electrical and thermal energy management of a residential energy hub, integrating demand response and energy storage system," *Energy Buildings*, vol. 90, pp. 65–75, Mar. 2015, doi: 10.1016/j.enbuild.2014.12.039.
[26] S. C. Kang, "Robust Linear optimization using distributional information," Ph.D. dissertation, Boston Univ., Boston, MA, USA, 2008.

MAO YUNSHOU received the B.E. degree in electrical engineering from the North University of China, Taiyuan, China, in 2013, and the M.E. degree from the Guangdong University of Technology, Guangzhou, China, in 2017, where he is currently pursuing the Ph.D. degree in electrical power engineering. His current research interests include integrated energy system planning and operation, multi-energy network operation, and optimization theory in these areas.

WU JIEKANG (Member, IEEE) was born in China, in December 1965. He received the degrees (Hons.) from Zhejiang University, the South China University of Technology, and Guangxi University. His employment experience included as an Engineer with Power Supply Bureau; an Engineer with Electrical Engineering Designing Institute; a Professor with Zhejiang University, Guangxi University, and the Guangdong University of Technology; and an Engineer in large enterprises. His research interest includes power systems with renewable energy.

WANG RUIDONG is currently with the School of Automation Engineering, Guangdong University of Technology, Guangzhou, China. His research interest includes renewable smart integrated energy system operation and analysis.

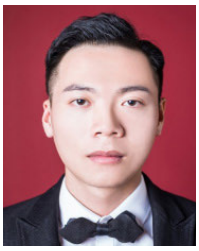

CAI ZHIHONG is currently with the School of Automation Engineering, Guangdong University of Technology, Guangzhou, China. His research interests include power system operation and planning and analysis.

CHEN LINGMIN is currently with Department of Experiment Teaching, Guangdong University of Technology, Guangzhou, Guangdong, China. Her research interest includes power system operation and control

ZHANG RAN is currently a Senior Engineer with Beijing Aerocim Technology Company Ltd., Beijing, China. His research interest includes complex network modeling in aerospace

ZHANG WENJIE is currently a Senior Engineer with Huizhou Power Supply Bureau, Guangdong Power Grid Corporation, Huizhou, China. His research interests include smart gird network operation and planning and analysis.